Journal of Heat and Mass Transfer Research 10 (2023) 135 - 146

Journal of Heat and Mass Transfer Research

Journal homepage: https://jhmtr.semnan.ac.ir

Semnan University

Review Article

Physical Overview of the Instability in Laminar Wall-Bounded Flows of Viscoplastic and Viscoelastic Fluids at Subcritical Reynolds Numbers

Hamed Mirzaee [*,a], Goodarz Ahmadi [b], Roohollah Rafee [a], Farhad Talebi [a]

[a] *Faculty of Mechanical Engineering, Semnan University, Semnan, Iran.*
[b] *Department of Mechanical and Aerospace Engineering, Clarkson University, Potsdam, NY, USA.*

PAPER INFO

Paper history:

Received: 2023-06-26
Revised: 2023-09-01
Accepted: 2023-09-01

Keywords:

Flow;
Instability;
Transition;
Perturbation;
Amplitude;
Non-Newtonian fluids.

ABSTRACT

This paper reviews the latest findings on instability and subcritical transition to turbulence in wall-bounded flows (i.e., pipe Poiseuille flow, plane channel flow, and plane Couette flow). Among the non-Newtonian fluids, viscoelastic and viscoplastic fluids were investigated. The main focus was on the early stage of transitional flow and the appearance of coherent structures. The scaling of threshold disturbance amplitude for the onset of natural transition was discussed. In addition, the transition of Newtonian fluids was compared with that of non-Newtonian fluids. Accordingly, the scaling for the transition of viscoelastic (i.e., highly elastic) fluid can be shown as $A_c=O(Wi^{\gamma})$, where Wi is the Weissenberg number, $\gamma \leq -1$ is a scaling constant, and A_c is the critical perturbation amplitude. Moreover, the viscoelastic fluid flow at high Re numbers (i.e., Re>>1) is more stable than the Newtonian fluid flow in terms of the critical disturbance magnitude. Interestingly, the scaling for instability of viscoplastic fluid can be read as $Re_c=O(Bi^{\beta})$, where Bi is the Bingham number and $\beta \leq 1$ is a constant. It was noted that exploration of perturbations like vortices, streaks, and traveling waves together with their amplitudes could clarify the instability and transition process. Hence, this paper focused on physical behavior and realizations of the transitional flow. Finally, a summary of consequential implications and some open issues for future works were presented and discussed.

DOI: 10.22075/jhmtr.2023.31061.1455

1. Introduction

Gotthilf Hagen, a hydraulic and civil engineer, was the first to realize and think about the transition to turbulence in his study of pipe flow (see Eckert [1]). Almost 30 years later, in 1883, Osborne Reynolds experimentally noticed that the Poiseuille flow in pipe remains stable to small disturbances up to the value of UD/ν (later called Reynolds number, Re) equals 13000 in some experiments. Years later, Ekman [2] reached the value of 50000 utilizing Reynolds' authentic setup in more refined experiments. Thus, this type of flow was stable for each Re>>1 if he decreased the vibration of the experimental apparatus and disturbances of the incoming flow further. Observations of Pfenniger [3] and the linear stability analysis also admitted this is the case (e.g., see Kundu and Cohen, [4]). It is noteworthy that Meseguer & Trefethen [5] showed that this flow remains linearly stable up to $Re=10^7$ if there is no disturbance. However, it is known that the pipe flow becomes unstable for certain small disturbances as the Re number approaches 2000. Since 2000>>1 physically, this contradiction should be somehow addressed in fluid mechanics, and the minimum amplitude of disturbance for the onset of transition should be established.

[*] *Corresponding Author: Hamed Mirzaee.*
Email: h.mirzaee@alum.semnan.ac.ir ; h.mirzaee.mec@gmail.com

The perturbed state can be regarded as the summation of the basic or unperturbed state and perturbation. The temporal instability means the amplitude of perturbation introduced in the flow field grows exponentially. A system is considered unstable even if one mode of disturbance grows exponentially (Chandrasekhar [6]).

Subcritical transition signifies that a fluid flow goes through a transition to turbulence at a Reynolds number which is much less than the prediction of linear stability theory (John et al. [7]). In other words, such a flow is nonlinearly unstable to finite-amplitude perturbation. For convenience, the first results of linear stability analysis for pipe Poiseuille flow, channel flow, and plane Couette flow of Newtonian fluids are listed in Table 1.

Table 1. Early studies on linear stability analysis for Newtonian fluids subject to small-amplitude disturbances**.**

Flow type	Effective parameter	Critical value	Reference
Plane Couette	Re	Re→∞	Romanov [26]
Plane channel/Plane Poiseuille	Re	Re=5772	Orszag [29]
Pipe Poiseuille	Re	Re→∞	Davey & Drazin [31]

For Non-Newtonian fluids, the variations of shear stress versus the shear rate are not linear and/or do not initiate from the origin. The apparent or effective viscosity for any point of a nonlinear curve is defined as the slope at that point (White [8]). It is emphasized that the apparent viscosity is not a true material constant (Leal [9]). The non-Newtonian fluids are rheological classified into three groups: generalized Newtonian fluids (GNF), time-dependent fluids, and viscoelastic fluids. Table 2 shows the division according to Chhabra & Richardson [10]. Behaviors of GNFs against the strain rate and time-dependent fluids against time are depicted in Fig. 1. Moreover, behaviors of viscoelastic fluids are such that after deformation, they return to their "recent" equilibrium state partly and, in this sense, resemble elastic solids (Leal [9]). However, it is not appropriate to categorize a fluid as a Newtonian or non-Newtonian fluid before considering the flow conditions. For example, a Newtonian liquid with small molecules like water under a very high shear rate may exhibit a shear-thinning feature or a polymeric liquid can be regarded as a Newtonian liquid under a very low shear rate (Leal [9]). It is worth mentioning that a polymer solution (i.e., a viscoelastic fluid) with the coiled-up conformation has lesser viscosity than that with the stretched conformation and exhibits the shear-thinning behaviour even at low concentrations (Draad et al. [11]).

Masuda et al. [12] were the first to suggest the addition of nanoparticles to a carrier fluid for making a new fluid with enhanced thermophysical properties. Pak and Cho [13] showed that the solution of water-based nanofluid with 13nm Al_2O_3 particles exhibits shear-thinning behaviour at nearly 3% volume fraction. Besides, Mirzaee et al. [14] rigorously compared the important available models for evaluating nanofluid dynamic viscosity and presented an accurate correlation for the viscosity of water-Al_2O_3 for 20nm particles. The effect of temperature-dependent viscosity in a pipe flow was examined by Ellahi [15]. Furthermore, Majeed et al. [16] studied the heat transfer of a magnetic nanofluid flowing over a stretching sheet. It was shown graphically that an increment of viscoelasticity restricts fluid motion near the sheet and aids the fluid motion away from it. Shaheen et al. [17] used asymptotic methods to study the cilia-assisted flow of the viscoelastic mucus flow in a tube. It was portrayed that the axial velocity decelerated by raising the viscoelastic material parameter, i.e., relaxation time. Bhatti et al. [18] dealt with the cilia-assisted flow of a Sutterby viscoelastic fluid inside an axisymmetric channel. Accordingly, fluctuations in the velocity profile were depicted for differing physical parameters, e.g., cilia length and orientation. Mehdizadeh et al. [19] simulated and compared different non-Newtonian models inside a cavity flow. Accordingly, variation of velocities utilizing various models did not collapse into a single curve. Nemati et al. [20] considered the effect of heat absorption/generation in a cavity on some non-Newtonian fluids' natural convection. Accordingly, heat absorption and generation positively and negatively impact the Nusselt number, respectively.

Table 2. Classification of non-Newtonian fluids according to their rheological behaviors

Non-Newtonian fluids						
Time-independent or generalized Newtonian fluids (GNF)			**Time-dependent fluids**		**Viscoelastic fluids**	
Shear-thinning or pseudoplastic fluids	Shear-thickening or dilatant fluids	Viscoplastic fluids	Thixotropic fluids	Rheopectic or anti-thixotropic fluids	Linear viscoelastic fluids	Nonlinear viscoelastic fluids

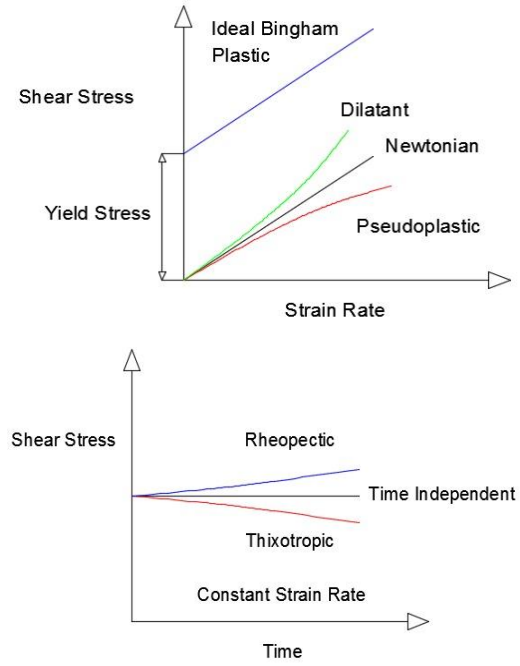

Fig. 1. Behaviors of GNFs (up) and time-dependent fluids (down) [8].

The primary motivation for the present study was to review subcritical and critical transitions in pipe flow, channel flow, and plane Couette flow and summarize the latest significant physical (empirical) and numerical findings concerning the transitional flow. This review article would be of interest to physicists, mathematicians, and engineers interested in the field of instability in non-Newtonian fluid dynamics.

This study mainly reviews the literature concerning the subcritical and critical transition from 2002 onwards from the physical perspective with some references to seminal older papers. It should be stressed that this review article does not include the transition from the dynamical systems viewpoint.

The review article was arranged as follows: Section 1 introduces the historical and early works concerning the transition in wall-bounded flows of Newtonian fluids and presents a classification of non-Newtonian fluids. Next, the instability of viscoplastic fluids is treated in Section 2 and its subsections. Afterward, the instability of viscoelastic fluids is discussed in Section 3 and its subsections. Finally, concluding remarks and some open issues for future research are described in the conclusion section.

2. Viscoplastic Fluids

Viscoplastic fluids have some applications in natural resource industries, such as the drilling and cementing of oil wells. It should be noted that a Newtonian fluid is obtained for the case of Bingham fluid and vanishing yield stress. In this section, the transition of viscoplastic (also known as the yield stress fluids) is described. For convenience, the results of linear stability analysis for pipe Poiseuille flow, channel flow, and plane Couette flow of Bingham fluids are listed in Table 3.

2.1. Governing Equations

The governing equations for Bingham fluids are written as (Bingham [21]):

$$\nabla \cdot \vec{u} = 0 \tag{1}$$

$$\rho \frac{\partial \vec{u}}{\partial t} + \rho(\vec{u} \cdot \nabla \vec{u}) = -\nabla p + \nabla \cdot \bar{\bar{\tau}} \tag{2}$$

$$\bar{\bar{\tau}} = 2\left(\frac{\tau_Y}{2\dot{\gamma}} + \mu_P\right)\bar{\bar{\dot{\gamma}}} \quad if \quad \tau \geq \tau_Y \tag{3}$$

$$\bar{\bar{\dot{\gamma}}} = 0 \quad if \quad \tau < \tau_Y \tag{4}$$

$$\eta(\dot{\gamma}) = \frac{\tau_Y}{2\dot{\gamma}} + \mu_P \tag{5}$$

$$\bar{\bar{\tau}} = 2\eta\bar{\bar{\dot{\gamma}}} \tag{6}$$

where $\bar{\bar{\tau}}$ is the stress tensor, τ_Y is the magnitude of yield stress, $\bar{\bar{\dot{\gamma}}}$ is the strain rate tensor $(\dot{\gamma}_{ij} = \frac{1}{2}\left(\frac{\partial u_i}{\partial x_j} + \frac{\partial u_j}{\partial x_i}\right))$, $\tau = \sqrt{2\tau_{ij}\tau_{ij}}$ is the magnitude of the stress tensor (for the concept of tensor notation, see Mase [22]), and μ_P is the plastic viscosity (equal to the zero-shear-rate viscosity) of the yielded fluid, and η is the effective or apparent viscosity, $\dot{\gamma} = \sqrt{2\dot{\gamma}_{ij}\dot{\gamma}_{ij}}$ is magnitude of the strain rate tensor. Here, note that the Reynolds number is defined as $Re = \frac{\rho U_0 L_0}{\mu_p}$ where is the U_0 characteristic velocity and L_0 is the characteristic length and $Bi = \frac{\tau_Y L_0}{\mu_p U_0}$ is the Bingham number.

Table 3. Early studies on linear stability analysis under small-amplitude disturbances for Bingham fluids.

Flow type	Wall type	Effective parameter(s)	Critical value(s)	Reference
Plane Couette	Rigid	Re, Bi	Inner critical Re (i. e. Re_1) increases with Bi/ β where β=1-Re_2/Re_1	Graebel [27] Note: the author analytically studied Taylor-Couette flow in a thin gap.
Plane channel / Plane Poiseuille	Rigid	Re, Bi	Critical Re increases with Bi (e.g., Re=9034 for Bi=38)	Frigaard et al. [30]
Pipe Poiseuille	Rigid	Re, Bi	Re_c=O($Bi^{0.5}$) as Bi→∞	Nouar & Frigaard [34] Note: the authors assumed linear stability.

For the Herschel-Bulkley model, the stress tensor and the effective viscosity are given by (Bird et al. [23]):

$$\bar{\bar{\tau}} = 2\left(\frac{\tau_Y}{2\dot{\gamma}} + k\dot{\gamma}^{n-1}\right)\bar{\bar{\dot{\gamma}}} \quad if \quad \tau \geq \tau_Y \tag{7}$$

$$\bar{\bar{\dot{\gamma}}} = 0 \quad if \quad \tau < \tau_Y \tag{8}$$

$$\eta(\dot{\gamma}) = \frac{\tau_Y}{2\dot{\gamma}} + k\dot{\gamma}^{n-1} \tag{9}$$

$$\bar{\bar{\tau}} = 2\eta\bar{\bar{\dot{\gamma}}} \tag{10}$$

here, k is the consistency index, and n < 1 is the shear-thinning power-law exponent. Note that the Reynolds number is defined as $Re = \frac{\rho U_0^2}{k(U_0/L_0)^n}$ and $Hb = \frac{\tau_Y}{k(U_0/L_0)^n}$ is the Herschel-Bulkley number.

The amplitude of perturbation velocity is defined as (Chapman [33]):

$$\left|\overrightarrow{u'}\right| = E^{1/2} = \left(\frac{1}{2V}\int\left(u'^2 + v'^2 + w'^2\right)dV\right)^{1/2} \tag{11}$$

where E is the perturbation kinetic energy, and V is a periodic volume of fluid.

Moreover, the relative or non-dimensional perturbation velocity is given by:

$$\left|\overrightarrow{u'}\right|^* = \frac{\left|\overrightarrow{u'}\right|}{U_0} \tag{12}$$

Note that Eq. (12) can be used for the external disturbance imposed on the flow through a hole/slot or holes/slots on the wall, with the numerator treated as the average disturbance velocity over the hole or slot surface area.

In this paragraph, the general solution methodology is presented concisely. The normal mode method is utilized for linear stability analysis. The perturbed state consists of a basic or unperturbed state plus sinusoidal perturbations imposed on the basic state ($\vec{u} = \vec{U} + \vec{u}'$).

Assume $\vec{U} = (U(y), 0, 0)$ is the basic state and $u'(x, y, z, t) = Real(\hat{u}(y)e^{i(k_x + k_z - \omega t)})$ is the perturbation. Here, $\hat{u}(y) = \hat{u}_r(y) + i\hat{u}_i(y)$ is the complex amplitude, $\omega = \omega_r + i\omega_i$ is the complex frequency, and k_x is streamwise wavenumber and k_z is the spanwise wavenumber respectively. After writing the other variables as the summation of basic state and perturbation and inserting them in the Navier-Stokes equations, ignoring the product of small perturbations, and eliminating the pressure term, the so-called Orr-Sommerfeld equation is obtained. This forms an eigenvalue problem for ω. The system is stable to the prescribed wavenumbers, if $\omega_i < 0$, and unstable to those, if $\omega_i > 0$. The case of $\omega_i = 0$ is termed marginal stability (Chandrasekhar [6]). There are various methods for computing the eigenvalue and its eigenfunctions. One method is based on a variational principle which produces nearly accurate results. The other method is the use of asymptotic expansion or WKBJ theory, which produces a good approximation. Moreover, there exist three numerical methods for treating this eigenvalue problem. These methods are 1) expansions in orthogonal functions and use of QR matrix eigenvalue algorithm, 2) finite difference methods and utilizing an iterative procedure, 3) initial-value methods (shooting technique) whereby the Orr-Sommerfeld equation is cast into a system of first-order differential equations (see Drazin and Reid [24]).

2.2. Comparison of Unstable Newtonian Versus Unstable Viscoplastic Fluids

Three models are typically utilized for the study of viscoplastic fluids. These models are the Bingham plastic model (the simplest one), the Herschel-Bulkley model, and the Casson model (Escudier [25]).

Plane Couette flow of Newtonian fluid was found stable to small disturbances for all values of Re (Romanov [26]). In contrast, the plane Couette flow of viscoplastic fluids exhibits instability on the thin gap limit (Graebel [27]). Moreover, Landry et al. [28] improved Graebel's study, presenting a better scaling as $Re_{1,c} \geq (k^2[1+O(Bi)+\pi^2)/(1-\eta)^{1/2}$ where $Re_{1,c}$, k and η are critical Re number of the inner cylinder, axial wavenumber, and radii ratio, respectively. As for Plane Poiseuille flow, Orszag [29] computed spectrally that the minimum critical Re number for Newtonian fluids equals 5772. However, Frigaard et al. [30] suggested that the critical Re number rises with an increment of the Bi number. They reported a critical Re number of about 9000 in a specific situation. Notably, Davey and Drazin [31] performed a series of numerical simulations and suggested that the pipe Poiseuille flow was stable to axisymmetric disturbances. It is worth mentioning that the linearized differential operator of Navier-Stokes equations is not self-adjoint or non-normal (Schmid and Henningson [32]). For this reason, spurious unstable modes were seen, and as a result, some of the earlier numerical computations were not fully resolved and successful (Chapman [33]). Finally, Nouar and Frigaard [34] explored the pipe Poiseuille flow of viscoplastic fluid. They used the linear stability analysis and presented a valuable scaling for the critical Re number asymptotically as $Re_c = O(Bi^{0.5})$ for high values of the Bi number.

2.3. Instability of Viscoplastic Fluids

Park et al. [35], for the first time, experimented to examine the velocity profile of a viscoplastic fluid flowing in a pipe. The experimental fluid was a transparent slurry containing 14 vol.% silica particles with a mean diameter of 1.79 μm. The transition region was 500 (1/s) <8U/D<650 (1/s). According to this experiment, the axial turbulence level at the centerline for the non-Newtonian fluid (4.7%) was much less than that for the Newtonian fluid (11%) during the transition. The turbulent velocity profile was almost the 1/7 power-law profile. In addition, the axial turbulence level in the fully-developed state near the wall was slightly greater than that for the Newtonian fluid.

Escudier and Presti [36] measured the flow mean velocity and turbulence level of a thixotropic liquid (water-based Laponite solution) in fully developed pipe flows. The Herschel-Bulkley model was utilized for the characterization of the rheological properties.

Noticeably, the velocity profiles showed an "asymmetry" before the transition. They linked the asymmetry to the instability of the plastic plug core. The thixotropy of the used fluid made the equilibrium (viscometric) effective viscosity differ from that computed from the measurement of near-wall mean velocities.

Frigaard et al. [37] predicted the transition of viscoplastic fluid flow in a plane channel and pipe. They used linear stability theory to achieve an upper bound for the critical Re number in terms of the Bingham number ($Bi = \frac{\tau_Y R}{\mu_p U}$). It was shown that available models predict different critical Re numbers for the practical range of 0<Bi<50. As an example, for pipe flow at Bi=0 all models yield $Re_c \approx 1100$ (here, Re is based on pipe radius), at Bi=10, the Hanks correlation [38; 39] and the Hedström [40] correlation, both give $Re_c \approx 3750$ whereas at Bi=20, the Hanks correlation gives $Re_c \approx 6200$ but the Hedström correlation gives $Re_c \approx 8700$.

Frigaard and Nouar [41] studied the linear stability of Bingham fluid in a 3-D channel. They reported that the bound of critical Re number is of form $Re=O(Bi^{3/4})$ as Bi>>1 and also Re=O(Bi) for long wavelengths, which were in agreement with 2-D disturbances due to Squire's theorem.

Peixinho et al. [42] planned an experiment to compare the laminar, transitional, and turbulent flow of a viscoplastic fluid (solution with 0.2 wt. % Carbopol), a shear-thinning fluid (solution with 0.2 wt. % CMC), and a Newtonian fluid (glucose syrup with a viscosity of 50 mPa.s) through a tube. First, it was shown that the shear stress-shear rate of the shear-thinning fluid exhibits three different regions (low shear rate region, intermediate region, and high shear rate region), and the entire range was described by the Cross model (Cross [43]). Defining $Re' = \frac{\rho U^{2-n'} D^{n'}}{8^{n'-1} k'}$ (with n' and k' being functions of the Herschel-Bulkley parameters) as a generalized Reynolds number, laminar flows were seen for Re'<2000. Based on their results (Fig. 2), a drastic decrease in the centerline velocity was observed for 2000<Re<3000 and the Newtonian case. The trend of the velocity of the shear-thinning fluid was similar to that of the Newtonian fluid. But, the transition of the viscoplastic fluid happened in three stages.

In the first stage (2550<Re'<3300), the normalized velocity decreases marginally, then in the second stage (3300<Re'<4000), the velocity drops drastically, and in the third stage (Re'>4000), the reduction of the velocity gets less severe. Noticeably, the asymmetric velocity profile was obtained for the viscoplastic fluid during the transition.

By analyzing the velocity signals at the center of the pipe, an isolated puff was detected in the second stage. It is worth noting that inside the puff, the plug zone was disturbed, and between the puffs, the plug zone existed. In addition, Peixinho et al. [42] mentioned that viscoplasticity and shear-thinning, both, augment the stability of the flow.

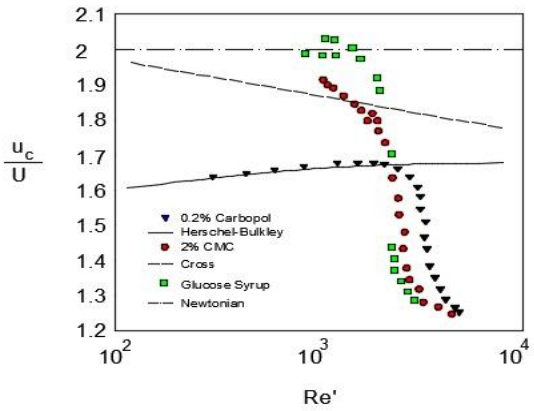

Fig. 2. The normalized velocity at the center of the pipe vs. the generalized Re number (Peixinho et al. [42]).

Nouar et al. [44] analyzed the linear stability of the plane Poiseuille flow of Bingham fluids. Accordingly, this flow remains stable to small amplitude disturbances. The optimal perturbations with the largest transient energy growth were streamwise vortices as Bi<<1. However, when Bi>1, the optimal perturbations were in the form of oblique vortices. It was argued that streamwise vortices attain energy by the lift-up mechanism, whereas the oblique vortices attain energy by the lift-up mechanism and the Reynolds stress in the wall-normal direction.

Esmael and Nouar [45] evaluated the transition of a yield stress fluid flow in a pipe numerically and experimentally. They achieved the asymmetry in the mean velocity profile during the transition, confirming the observations of Escudier and Presti [36]. Notably, the transitional flow exhibits a pair of counter-rotating vortices.

Figure 3 represents a pair of streamwise vortices and low-speed and high-speed axial streaks at a cross-section. Here, it is well worth defining the streamwise vortices and streaks from the physical point of view. According to Chapman [33], a streamwise vortex is an elongated region of vorticity approximately aligned with the basic laminar flow, while a streamwise streak is an elongated region of relatively higher or lower velocity approximately aligned with this flow.

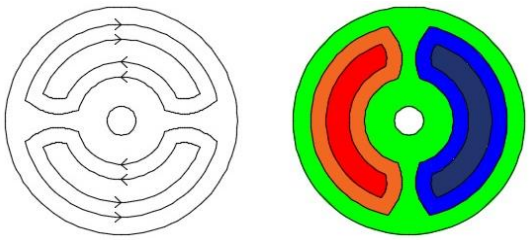

Fig. 3. Streamline plot of streamwise vortices (left) and contour of streamwise streaks (right). High-speed streaks are red, and low-speed streaks are blue (Esmael and Nouar [45]).

Guzel et al. [46] conducted experiments on three classes of visco-plastic fluids in a pipe. Using flow structure function as a statistical measure, they found that visco-plastic and shear-thinning fluids behave similarly. Further, it was postulated that the Reynolds

stresses break up the plug region away from the pipe wall before transition.

Liu and Liu [47] explored the linear stability of the pipe Poiesuille flow of a Bingham fluid. The critical energy Reynolds number scales like $Bi^{1/2}$. It is worth noting that the energy Re number is the Re number below which the disturbance kinetic energy does not grow and falls monotonically with time.

Bentrad et al. [48] examined the instability of the pipe Poiseuille flow of the Herschel-Bulkley fluid. It was discussed that the small-amplitude disturbances die out quickly. Based on this study, the optimal perturbations with the largest amplification of energy are streamwise, oblique, and axisymmetric vortices, respectively, for Hb<<1, Hb=O(1) (i.e., the finite values of Hb) and Hb>>1.

Singh et al. [49] analyzed the effect of yield stress on the turbulent statistics in the pipe flow employing the DNS. The yield stress varied from 0 to 20% of the wall shear stress. It was concluded that the mean streamwise velocity does not depend on the yield stress in the viscous sublayer. Also, the disturbance kinetic energy was affected by the yield stress for $y^+ \leq 60$.

Mitishital et al. [50] performed an experiment on the fully-developed turbulent flow of viscoplastic fluids (Carbopol solutions) in a channel with an aspect ratio of 2:1. The Reynolds number ranges from 9400 to 51000. The increment of streamwise fluctuation velocity and the decrement of wall-normal fluctuation velocity was captured, compared to the water flow at the same velocity. It was found that the energy of larger eddies of the Carbopol solution was greater than that of water, and the energy of smaller eddies decreased more rapidly than that of water. Further, it was disclosed that by raising the Re number, the streamwise energy spectrum of viscoplastic solution approaches that of water.

3. Viscoelastic fluids

Viscoelastic fluids have many applications in manufacturing industries, such as polymer processing, lubrication, and coating flows. Likewise, some bio-fluids, like blood, are viscoelastic. In this section, the transition of viscoelastic is described. For convenience, the results of linear stability analysis for pipe Poiseuille flow, channel flow, and plane Couette flow of viscoelastic fluids are listed in Table 4.

3.1. Governing Equations

The continuity equation is the same as Eq. (1), and the momentum equations for viscoelastic fluids are written as (Bird et al. [23]):

$$\rho \frac{\partial \vec{u}}{\partial t} + \rho(\vec{u} \cdot \nabla \vec{u}) = -\nabla p + \eta_s \nabla^2 \vec{u} + \nabla \cdot \bar{\bar{\tau}}_p \tag{13}$$

$$\frac{\partial \bar{\bar{c}}}{\partial t} + \vec{u} \cdot \nabla \bar{\bar{c}} = \bar{\bar{c}} \cdot \nabla \vec{u} + (\nabla \vec{u})^T \cdot \bar{\bar{c}} + D \nabla^2 \bar{\bar{c}} - \frac{\bar{\bar{\tau}}_p}{\eta_p} \tag{14}$$

$$\bar{\bar{\tau}}_p = \frac{\eta_p}{\lambda} \left(f(\bar{\bar{c}}) \bar{\bar{c}} - \bar{\bar{c}}_{eq} \right) \tag{15}$$

$$f(\bar{\bar{c}}) = 1 \quad \textit{for Oldroyd-B model} \tag{16}$$

$$f(\bar{\bar{c}}) = \frac{1}{1 - tr\bar{\bar{c}}/L^2} \quad \textit{for FENE-P model} \tag{17}$$

where η_s is the solvent viscosity, η_p is the contribution of polymers to the total viscosity, λ is the stress relaxation time, $\bar{\bar{\tau}}_p$ is the viscoelastic or polymer stress tensor, $\bar{\bar{c}} = \langle \vec{q}\vec{q} \rangle$ is the conformation tensor, $\vec{q}$ is the end-to-end vector linking two ends of a polymer molecule, $\langle \cdot \rangle$ means the phase-space average, $\bar{\bar{c}}_{eq} = \frac{k_B T}{H} \bar{\bar{I}}$ is the equilibrium state, H is the spring constant, k_B is the Boltzmann constant, T is the absolute temperature, $\bar{\bar{I}}$ is the identity tensor, D is the molecular diffusivity, $f(\bar{\bar{c}})$ is known as the Peterlin's function, L is the maximum extension or extensibility of the polymer molecular chains.

Note that the Reynolds number is defined as $Re = \frac{\rho U_0 L_0}{\eta}$ with $\eta = \eta_s + \eta_p$ being the zero-shear-rate total viscosity of the solution, and $Wi = \lambda |\nabla \vec{u}|$ is the Weissenberg number with $|\nabla \vec{u}|$ being the magnitude of the velocity gradient or a characteristic strain rate, and $De = \frac{\lambda}{L_0/U_0}$ is the Deborah number, $\beta = \frac{\eta_s}{\eta}$ is the ratio of viscosities, and $Sc = \frac{\eta}{\rho D}$ is the Schmidt number, which is usually very high, e.g., $Sc = O(10^6)$.

It is worth noting that the De number is sometimes used instead of the Wi number. However, the Wi number is suited for steady flows, whereas the De number is suited for unsteady flows (see Leal [9]; Tanner [51]).

Table 4. Early studies on linear stability analysis under small-amplitude disturbances for viscoelastic fluids

Fluid type	Flow type	Wall type	Effective parameter(s)	Critical value(s)	Reference
UCM (Upper-convected Maxwell)	Plane Couette	Rigid	Re, Wi	Stable at low Re and low Wi	Lee & Finlayson [53]
			Re, Wi	Stable at low Re and high Wi, Stable at high Re and low Wi	Renardy & Renardy [54]
	Plane channel/ Plane Poiseuille	Rigid	Re, E=Wi/Re	E=0.0025, Re>1400	Porteous & Denn [55]
			Re, E=Wi/Re	Stable at low Re	Ho & Denn [56]
	Pipe Poiseuille	Rigid	Re, λ (relaxation time of solution)	if λ/Re is greater than a critical value	Hansen [57]

Oldroyd-B	Plane Couette	Rigid	Re, Wi, β	Wi→∞, β =0.2	Kupferman [58]
	Plane channel/ Plane Poiseuille	Rigid	Re, E=Wi/Re, β	β=0.5, E=0.001, Re=4231	Sureshkumar & Beris [59]
	Pipe Poiseuille	Rigid	Re, λ (relaxation time of solution)	If λ/Re is greater than a critical value	Hansen [57]

3.2. Comparison of Unstable Newtonian Versus Unstable Viscoelastic Fluids

Three models are typically utilized for the study of viscoelastic fluids. These models are the upper-convected Maxwell (UCM) model (the simplest one), the Oldroyd-B model, and the finitely extensible nonlinear elastic-Peterlin (FENE-P) model (see Bird et al. [23]). Notably, the UCM model represents a pure polymeric liquid (exclusive of a solvent). Also, the Oldroyd-B model (with a linear spring force) does not have an upper bound for the extensibility of the polymer chain. In contrast, the FENE-P model (with a nonlinear spring force) considers the extensibility of the polymer chain. Here, it should be stressed that calculating the maximum length of the polymer chain (L), Wi number, and the solvent-to-polymer solution viscosity ratio (β) in an experiment is challenging (Dubief et al., [52]).

Since the UCM model is a special case of the Oldroyd-B model, the results of the latter model are treated here. As mentioned before, Romanov [26], using an asymptotic analysis and the solvability condition, showed that the plane Couette flow of Newtonian fluid is linearly stable. Despite some earlier studies that showed the false instability at a high Wi number, Kupferman [58] determined that the plane Couette flow of Oldroyd-B fluid is linearly stable. As for the plane Poiseuille flow, Orszag [29] computed the critical Re number of 5772 for Newtonian fluids. In contrast, Sureshkumar and Beris [59] reached the critical Re number of 4231 for the case of E=0.001 (where E=Wi/Re is the elasticity number) and semi-dilute solution with β=0.5. In light of the linear stability of pipe Poiseuille flow of Newtonian fluids (Davey and Drazin [31]), Hansen [57] theoretically argued that a dilute Oldroyd fluid is stable to small-amplitude disturbances provided that the stress relaxation time is small enough.

3.3. Instability of Viscoelastic Fluids

Datta et al. [79] reviewed the recent advancement in the viscoelastic instabilities in parallel and curved flows. They stated that the maximum drag reduction (MDR) asymptotic limit might be the boundary between Newtonian and elasto-inertial turbulence. However, this statement needs further research and approval.

Dubief et al. [52] reviewed the phenomenon of elasto-inertial turbulence (EIT) in pipe and channel flows. They set out that so far, the comparison of dynamics between numerical simulations and the experiments is based on statistics of drag and fluctuating pressure and velocity, not the emerging coherent structure. Hence, explaining the self-sustaining process (SSP) at the onset of transition may elucidate the connection between EIT and maximum drag reduction (MDR). It is noteworthy that EIT may have spanwise instead of streamwise coherent flow structures.

Draad et al. [11] performed pipe-flow experiments to analyze the stability of dilute polymer solution subject to external disturbance. The natural transition point using the tap water reaches Re=60000. Based on this study, a fully stretched or fresh polymer solution decreases the transition point to Re=8000, and a fully coiled-up or degraded polymer solution reduces the transition point to Re=30000. However, polymers had a stabilizing effect in the sense that the critical disturbing velocity was higher than that using tap water. On the other side, no delay in the transition was seen for the degraded polymer solution, but a delay in transition was seen for the fresh polymer solution (see Fig. 4). They remarked that delay in the transition is expected when Wi=1.

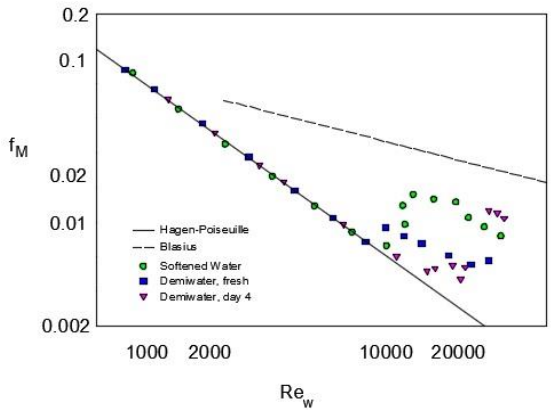

Fig. 4. The friction factor vs. Re number based on the viscosity at the wall for 20ppm polymer dissolved in softened and demineralized water. This graph illustrates transition without additional disturbance (Draad et al. [11]).

Escudier et al. [60] investigated the pipe flow of some aqueous polymer solutions. They stated that the transition was indistinguishable from the fraction factor-Re number plot; hence the root-mean-square axial fluctuation velocity near the pipe wall was utilized as an indicator. It was revealed that the polymer concentration had a trivial effect on the

critical Re number, and the transition ended at Re=5000 for most of the solutions.

Atalik and Keunings [61] analyzed the nonlinear stability of the plane channel and Couette flow of the Oldroyd-B fluid in both inertial and elastic regimes numerically. For plane channel flow, finite-amplitude periodic waves propagate beyond a critical Reynolds number in the inertial regime and quasi-periodic waves for viscosity ratio <0.01 in the elastic regime. As for plane Couette flow, oscillatory decay of finite-amplitude disturbances was seen at both regimes.

Govindarajan et al. [62] addressed the impact of viscosity variations on the stability of a simple channel flow. They reported that viscosity variations due to the presence of a small amount of polymers augment the threshold Re number five times (up to 31000). They argued that their finding could be related to the drag reduction encountered in turbulent dilute polymeric flows.

Meulenbroek et al. [63] suggested that viscoelastic fluid flow through a channel or tube exhibits nonlinear subcritical instability. They examined the UCM fluid. The instability begins at the Weissenberg number ($Wi = \lambda\dot{\gamma}$ where λ is the relaxation time) about 4 in a plane channel and 5.2 in the tube at zero Re number. Accordingly, the threshold amplitude of disturbances reduces with raising the Wi number (A_c=O(Wi^{-1})).

Morozov and van Saarloos [64] compared and contrasted the subcritical instability of visco-elastic and viscous parallel shear flows. They developed a criterion for instability of the visco-elastic parallel shear flows based on which the critical amplitude scales as $1/Wi^2$ (here, Wi is Weissenberg number, the ratio of normal stress difference to shear stress). It should be noted that this type of flow becomes turbulent at low Re numbers.

Hoda et al. [65] evaluated the energy amplification of the perturbed flow of Oldroyd-B fluid in a channel. The achievement of this study was that an increment of elasticity number could amplify the disturbance energy considerably, even at low Re numbers.

Li and Graham [66] studied the dynamics of drag reduction in the transitional regime (Re=3600) of dilute polymer solutions by DNS. They used the minimal flow unit (MFU) instead of a full-scale simulation of the plane channel flow. The transition happened in three stages, i.e., the pre-onset stage, the low-degree drag reduction stage, the high-degree drag reduction stage, and the maximum drag reduction (MDR) stage. The upper limit of the drag reduction was 26% and universal for the polymer parameters considered. Also, it was shown that the drag reduction begins at Wi=16 (see Fig. 5).

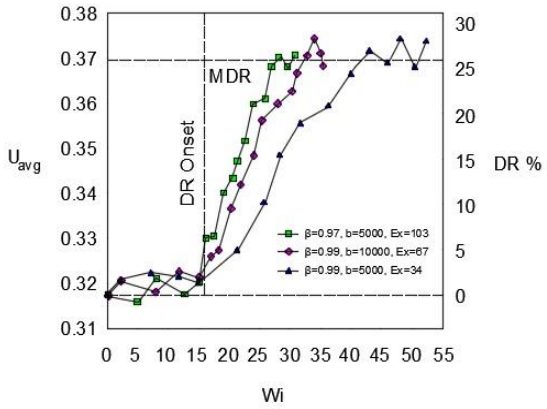

Fig. 5. Average streamwise velocity against Wi number. Here, b in the maximum stretching of polymer molecules (Li and Graham [66]).

Zhang et al. [67] numerically modeled the modal and non-modal (i.e., transient growth of disturbances) linear instability of the channel flow of Oldroyd-B and FENE-P fluids. It was found that the critical Re number happens at Wi. $\omega_r \approx 1$, where ω_r is the frequency of disturbance before transition. Likewise, it was shown that FENE-P fluid is more stable for lower values of β and more stable than Oldroyd-B fluid at high values of Wi number (Wi>5).

Samanta et al. [68] introduced elasto-inertial turbulence for viscoelastic fluid flow inside a pipe. Here, the elasto-inertial turbulence refers to the case that both Re and Wi numbers are nonzero and finite. They performed both experiments and direct numerical simulations. It was reported that dilute polymeric solution (with a concentration of less than 200 ppm) exhibits delayed transition. In contrast, dense solution (with concentrations equal to or greater than 200 ppm) exhibits early transition compared with the Newtonian case. Note that this observation was also held for finite-amplitude perturbations.

Garg et al. [69] reported for the first time the linear instability analysis of a viscoelastic fluid in pipe flow. The Oldroyd-B constitutive equation was adopted for the elastic stress tensor. It was demonstrated that instability is absent for Upper Convected Maxwell (UCM) model, i.e., β=0 (β is the viscosity ratio). Asymptotically, Re_c is of order $(1-\beta)^{-3/2}$ as β tends to unity and order $\beta^{-1/4}$ when it goes to zero.

Following the work of Garg et al. [69], Page et al. [70] computed the exact traveling wave solution of polymeric fluid in a channel. It was found that these solutions are arrowhead structures underpinning the elasto-inertial turbulence. Accordingly, the first unstable mode manifests itself at (Re, Wi, k) almost equals (50, 25, 2). Here, Wi and k are the Weissenberg number and streamwise wavenumber, respectively. Figure 6 illustrates the traveling waves of a viscoelastic fluid flow in a 2-D channel.

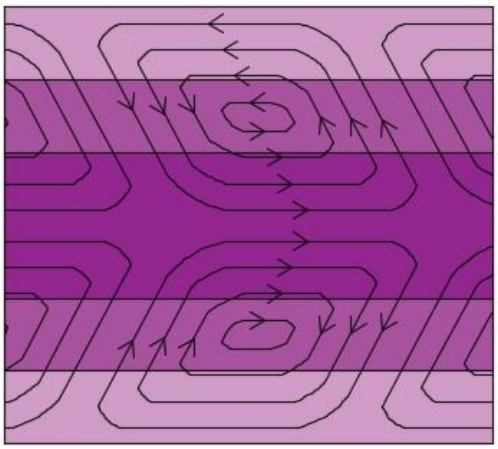

Fig. 6. A sample of traveling waves of viscoelastic fluid flow in a channel. Lines show the perturbation stream functions, and contours disclose the trC/L^2, with C being the conformation tensor and L being the maximum extensibility of polymer chains (Page et al. [70]).

Morozov and van Saarloos [71] examined the nonlinear instability of Oldroyd-B fluid in plane Poiseuille flow by asymptotic analysis. The results were reported for small Re numbers and β=0.05. Accordingly, the critical Wi number for the onset of the chaotic state was nearly 3. Moreover, streamwise vortices and spanwise streaks were illustrated.

Shekar et al. [72] simulated the 2-D plane Poiseuille flow of a dilute viscoelastic fluid at the Re=3000 by DNS. Based on this work, the elasto-inertial instability or a linear traveling wave was captured at Wi=13, and a nonlinear viscoelastic traveling wave came into existence at Wi=6.

Chaudhary et al. [73] used the linear stability analysis and showed that Oldroyd-B fluid in pipe flow subjected to the small axisymmetric disturbance is linearly unstable. They assessed the interplay of three non-dimensional numbers, i.e., Reynolds number (Re), elasticity number (E), and solvent-to-mixture viscosity ratio (β), on the onset of instability. It was argued that the Re_c scale with $(E(1-\beta))^{-3/2}$ in the limit of $E(1-\beta)<<1$. Note that their results did not agree well with the experimental values of Chandra et al. [74] in terms of minimal critical number prediction.

Wan et al. [75] used the weakly nonlinear analysis to examine the bifurcation type of neutral stability curve of visco-elastic pipe flow of Oldroyd-B fluid. They found at β >0.785, the bifurcation is subcritical, and at β<0.785, it is supercritical. Here β signifies the solvent-to-solution viscosity ratio. Their results were not in complete agreement with the experimental values of Samanta et al. [68].

Sanchez et al. [76] presented a detailed review of the utility of the Oldroyd-B model (the second model introduced by James Oldroyd in 1950) for predicting viscoelastic flow instability. They believed this model is simple but realistic and can still be used for predicting new instabilities in viscoelastic fluid states.

Buza et al. [77] examined the recently-found center mode instability of dilute polymeric fluid flow in a channel using weakly nonlinear analysis. The FENE-P fluid was utilized rather than Oldroyd-B fluid to account for finite polymer extension length. They clearly showed that instability is subcritical for Re<<1. Likewise, the FENE-P model is much more unstable than the Oldroyd-B model in the inertia-less case. In addition, they showed that its instability is either subcritical (for Wi<40) or supercritical (for Wi>40) when Re is nonzero and finite (i.e., Re=O(1)).

Dong and Zhang [78] performed an asymptotic analysis on instability in a viscoelastic pipe flow. Corroborating the Chaudhary et al. [73] study, they found three-layered unstable structures in the radial direction.

Conclusions and Recommendations

This paper reviewed the papers on the onset of transition to turbulence in parallel wall-bounded shear flows of viscoplastic and viscoelastic fluids, mainly in the last two decades. Furthermore, the important experimental and numerical results for the beginning of instability and natural transition were described. Accordingly, the available models for predicting the critical Re number for the viscoplastic fluid flow differ significantly, and a certain criterion is lacking in the literature for evaluating the threshold amplitude that could initiate transition in such flows. As for viscoelastic fluids, it was said that at high shear rates and Re numbers, the instability sets in at lower Re numbers than Newtonian instability. This case was termed elasto-inertial instability. In addition, the different scalings of threshold amplitude of perturbation in terms of Wi number were mentioned. From the above review and discussions, the following conclusion can be drawn:

- During transition, small-amplitude perturbations propagating in the flow can grow into finite-amplitude perturbations.
- Asymmetry in the velocity profile is a precursor of the unstable pipe flow of a viscoplastic fluid (Peixinho et al. [42]).
- Transition to turbulence in viscoplastic fluids arises when the Reynolds stresses overcome the yield stress (Guzel et al. [46]).
- The pipe flow of Newtonian fluid is stable to axisymmetric small-amplitude disturbances with zero azimuthal wavenumbers (Davey & Drazin [31]), while the pipe flow of dilute polymeric fluid is not (Garg et al. [69]).
- In the flow of dilute viscoelastic fluids through a channel, decreasing the polymer extension length (L_{max}) has a destabilizing effect as Re→0 and a stabilizing effect as Re is finite based on the marginal stability curves in the Re-Wi plane (Buza et al. [77]).

Based on these results, the recommendations for future works are as follows:

- Puffs (i.e., localized perturbation structures emerging in the transitional pipe flow) were not detected in the transitional flow of viscoelastic fluid of moderate concentration (greater than 200 ppm) in experiments of Samanta et al. [68]. Additional experimental observations and direct numerical simulations are needed for further clarification.
- The relationship among the elasto-inertial instability, the polymer concentration, and the ratio of solvent-to-solution viscosity need to be studied and quantified by experiment or DNS.
- Scaling laws for the minimum amplitude of disturbances for the onset of the elasto-inertial instability in viscoelastic fluid flow inside pipes and channels should be established.

Conflicts of Interest

The author declares that there is no conflict of interest regarding the publication of this manuscript. In addition, the authors have entirely observed the ethical issues, including plagiarism, informed consent, misconduct, data fabrication and/or falsification, double publication and/or submission, and redundancy.

References

[1] Eckert, M., 2021. Pipe flow: a gateway to turbulence. Arch. Hist. Exact Sci., 75, pp. 249–282.

[2] Ekman, V.W., 1911. On the change from steady to turbulent motion of liquids. Ark. Mat. Astron. Fys., 6(12), pp. 1–16.

[3] Pfenniger, W., 1961. Transition in the inlet length of tubes at high Reynolds numbers. In Boundary Layer and Flow Control, ed. GV Lachman, (pp. 970–80), New York: Pergamon.

[4] Kundu, P.K. and Cohen, I.M., 2008. Fluid mechanics. 4th ed.. Kidlington: Academic Press.

[5] Meseguer, A. and Trefethen, L.N., 2003. Linearized pipe flow to Reynolds number 10^7. J. Comput. Phys., 186 (1), pp. 178-197.

[6] Chandrasekhar, S., 1961. Hydrodynamic and hydromagnetic stability. Clarendon Press.

[7] John M.O., Obrist, D. and Kleiser, L., 2016. Secondary instability and subcritical transition of the leading-edge boundary layer. J. Fluid Mech., 792, pp. 682 – 711.

[8] White, F.M., 2006. Viscous Fluid Flow. 3rd ed. . New York: McGraw-Hill.

[9] Leal, L.G., 2007. Advanced transport phenomena: fluid mechanics and convective transport processes. Cambridge University Press.

[10] Chhabra, R.P. and Richardson, J.F., 2008. Non-Newtonian flow and applied rheology: engineering applications. Oxford: Butterworth-Heinemann.

[11] Draad, A.A., Kuiken, G.D.C. and Nieuwstadt, F.T.M., 1998. Laminar–turbulent transition in pipe flow for Newtonian and non-Newtonian fluids. J. Fluid Mech., 377, pp. 267-312.

[12] Masuda H., Ebata A. and Teramae K., 1993. Alteration of Thermal Conductivity and Viscosity of Liquid by Dispersing Ultra-Fine Particles (Dispersion of Al2O3, SiO2 and TiO2). Netsu Bussei., 7 (4), pp. 227-233.

[13] Pak B.C. and Cho Y.I., 1998. Hydrodynamic and heat transfer study of dispersed fluids with submicron metallic oxide particles. Exp. Heat Transf., 11, pp. 151-170.

[14] Mirzaee, H., Rafee, R., Rashidi, S. and Valipour, M.S., 2023. Two-phase modeling of low-Reynolds turbulent heat convection of Al2O3-water nanofluid in a 2-D helically corrugated channel. Chemical Engineering Communications, 210(4), pp. 634-654.

[15] Ellahi, R., 2013. The effects of MHD and temperature dependent viscosity on the flow of non-Newtonian nanofluid in a pipe: Analytical solutions. Applied Mathematical Modelling, 37, pp. 1451–1467.

[16] Majeed, A., Zeeshan, A., Alamri, S.Z. and Ellahi, R., 2018. Heat transfer analysis in ferromagnetic viscoelastic fluid flow over a stretching sheet with suction. Neural Comput. & Applic., 30, pp. 1947-1955.

[17] Shaheen, S., Maqbool, K., Ellahi, R. and Sait, S.M., 2021. Metachronal propulsion of non-Newtonian viscoelastic mucus in an axisymmetric tube with ciliated walls. Commun. Theor. Phys, 73(3), p.035006.

[18] Bhatti, M.M., Ishtiaq, F., Ellahi, R. and Sait, S.M., 2023. Novel Aspects of Cilia-Driven Flow of Viscoelastic Fluid through a Non-Darcy Medium under the Influence of an Induced Magnetic Field and Heat Transfer. Mathematics, 11(10), 2284.

[19] Mehdizadeh, A., Rahmati, A. and Sheikhzadeh, G., 2021. Simulation and comparison of non-Newtonian fluid models using LBM in a cavity. Journal of Heat and Mass Transfer Research, 8(1), pp. 115-125.

[20] Nemati, M., Sefid, M. and Rahmati, A., 2021. Analysis of the effect of periodic magnetic field, heat absorption/generation and aspect ratio of the enclosure on non-Newtonian natural convection. Journal of Heat and Mass Transfer Research, 8(2), pp. 187-203.

[21] Bingham, E.C., 1922. Fluidity and plasticity. McGraw-Hill.

[22] Mase, G.E., 1970. Schaum's Outline of Theory and Problems of Continuum mechanics. New York: McGraw-Hill.

[23] Bird, R.B., Armstrong, R.C. and Hassager, O., 1987. Dynamics of polymeric liquids, Vol. 1: Fluid mechanics. John Wiley & Sons.
[24] Drazin, P.G. and Reid, W.H., 2004. Hydrodynamic stability. Cambridge university press.
[25] Escudier, M., 2017. Introduction to Engineering Fluid Mechanics, 1st ed., Oxford University Press.
[26] Romanov, V.A., 1972. Stability of plane-parallel Couette flow. Funct. Anal. Applics., 7, pp. 137–146.
[27] Graebel, W. P., 1964. The hydrodynamic stability of a Bingham fluid in Couette flow. In M. Reiner & D. Abir (Eds.), Proceedings of International Symposium on 2nd Order Effects in Elasticity, Plasticity and Fluid Dynamics, Haifa, Israel, April 23–27, 1962, (pp. 636–649), New York: Macmillan.
[28] Landry, M. P., Frigaard, I. A. and Martinez, D. M., 2006. Stability and instability of Taylor–Couette flows of a Bingham fluid. J. Fluid Mech., 560, pp. 321-353.
[29] Orszag, S. A., 1971. Accurate solution of the Orr-Sommerfeld stability equation. J. Fluid Mech., 50(4), pp. 689-703.
[30] Frigaard, I.A., Howison, S.D. and Sobey, I.J., 1994. On the stability of Poiseuille flow of a Bingham fluid. J. Fluid Mech., 263, pp. 133-150.
[31] Davey, A. and Drazin, P.G., 1969. The stability of Poiseuille flow in a pipe. J. Fluid Mech., 36, pp. 209-218.
[32] Schmid, P.J. and Henningson, D.S., 2001. Stability and Transition in Shear Flows. New York: Springer.
[33] Chapman, S.J., 2002. Subcritical transition in channel flows. J. Fluid Mech., 451, pp. 35-97.
[34] Nouar, C. and Frigaard, I.A., 2001. Nonlinear stability of Poiseuille flow of a Bingham fluid: theoretical results and comparison with phenomenological criteria. J. Non-Newton. Fluid Mech., 100, pp. 127–149.
[35] Park, J.T., Mannheimer, R.J., Grimley, T. A. and Morrow, T.B., 1989. Pipe flow measurements of a transparent non-Newtonian slurry. J. Fluids Eng., 111(3), pp. 331-336.
[36] Escudier, M. P. and Presti, F., 1996. Pipe flow of a thixotropic liquid. J. Non-Newton. Fluid Mech., 62(2-3), pp. 291-306.
[37] Frigaard, I.A. and Nouar, C., 2003, April. Predicting Transition to Turbulence in Well Construction Flows, In SPE Latin American and Caribbean Petroleum Engineering Conference, Port-of-Spain, Trinidad and Tobago.
[38] Hanks, R. W., 1963. The laminar-turbulent transition for fluids with a yield stress. A.I.Ch.E. (Am. Inst. Chem. Engrs.) J., 9, TID-16087.
[39] Hanks, R. W., 1967. On the flow of Bingham plastic slurries in pipes and between parallel plates. Soc. Pet. Eng. J., 7(04), pp. 342-346.
[40] Hedström, B.O., 1952. Flow of plastic materials in pipes. Ind. Eng. Chem., 44(3), pp. 651-656.
[41] Frigaard, I.A. and Nouar, C., 2003. On three-dimensional linear stability of Poiseuille flow of Bingham fluids. Phys. Fluids, 15, 2843.
[42] Peixinho, J., Nouar, C., Desaubry, C. and Théron, B., 2005. Laminar transitional and turbulent flow of yield stress fluid in a pipe. J. Non-Newton. Fluid Mech., 128(2-3), pp. 172-184.
[43] Cross, M.M., 1965. Rheology of non-Newtonian fluids: a new flow equation for pseudoplastic systems. J. colloid sci., 20(5), pp. 417-437.
[44] Nouar, C., Kabouya, N., Dusek, J. and Mamou, M., 2007. Modal and non-modal linear stability of the plane Bingham–Poiseuille flow. J. Fluid Mech., 577, pp. 211-239.
[45] Esmael, A. and Nouar, C., 2008. Transitional flow of a yield-stress fluid in a pipe: Evidence of a robust coherent structure. Phys. Rev. E, 77(5), 057302.
[46] Guzel, B., Burghelea, T., Frigaard, I.A. and Martinez, D.M., 2009. Observation of laminar–turbulent transition of a yield stress fluid in Hagen–Poiseuille flow. J. Fluid Mech., 627, pp. 97–128.
[47] Liu, R. and Liu, Q. S., 2014. Non-modal stability in Hagen-Poiseuille flow of a Bingham fluid. Phys. Fluids, 26(1), 014102.
[48] Bentrad, H., Esmael, A., Nouar, C., Lefevre, A. and Ait-Messaoudene, N., 2017. Energy growth in Hagen–Poiseuille flow of Herschel–Bulkley fluid. J. Non-Newton. Fluid Mech., 241, pp. 43-59.
[49] Singh, J., Rudman, M., Blackburn, H.M., 2017. The effect of yield stress on pipe flow turbulence for generalised Newtonian fluids. J. Non-Newton. Fluid Mech., 249, pp. 53-62.
[50] Mitishita, R.S., MacKenzie, J. A., Elfring, G.J. and Frigaard, I.A., 2021. Fully turbulent flows of viscoplastic fluids in a rectangular duct. J. Non-Newton. Fluid Mech., 293, 104570.
[51] Tanner, R.I., 2000. Engineering rheology. 2nd ed. Oxford University Press.
[52] Dubief, Y., Terrapon, V. E. and Hof, B., 2023. Elasto-inertial turbulence. Annu. Rev. Fluid Mech., 55.
[53] Lee, K.-C. and Finlayson, B.A., 1986. Stability of plane Poiseuille and Couette flow of a Maxwell fluid. J. Non-Newton. Fluid Mech., 21 (1), pp. 65–78.
[54] Renardy, M. and Renardy, Y., 1986. Linear stability of plane Couette flow of an upper convected Maxwell fluid. J. Non-Newton. Fluid Mech., 22, pp. 23–33.
[55] Porteous, K.C. and Denn, M.M., 1972. Linear stability of plane Poiseuille flow of viscoelastic liquids. Trans. Soc. Rheol., 16 (2), pp. 295–308.

[56] Ho, T.C. and Denn, M.M., 1977. Stability of plane Poiseuille flow of a highly elastic liquid. J. Non Newton. Fluid Mech., 3 (2), pp. 179–195.
[57] Hansen, R., 1973. Stability of laminar pipe flows of drag reducing polymer solutions in the presence of high-phase-velocity disturbances. AIChE J., 19 (2), pp. 298–304.
[58] Kupferman, R., 2005. On the linear stability of plane Couette flow for an Oldroyd-B fluid and its numerical approximation. J. Non-Newton. Fluid Mech., 127, pp. 169–190.
[59] Sureshkumar, R. and Beris, A.N., 1995b. Linear stability analysis of viscoelastic Poiseuille flow using an Arnoldi-based orthogonalization algorithm. J. Non-Newton. Fluid Mech., 56 (2), pp. 151–182.
[60] Escudier, M.P., Presti, F. and Smith, S., 1999. Drag reduction in the turbulent pipe flow of polymers. J. non-Newton. Fluid Mech., 81(3), pp. 197-213.
[61] Atalik, K. and Keunings, R., 2002. Non-linear temporal stability analysis of viscoelastic plane channel flows using a fully-spectral method. J. Non-Newton. Fluid Mech., 102, pp. 299-319.
[62] Govindarajan, R., L'vov, V.S., Procaccia, I. and Sameen, A., 2003. Stabilization of Hydrodynamic Flows by Small Viscosity Variations. Phys. Rev. E, 67, 026310.
[63] Meulenbroek, B., Storm, C., Morozov, A.N. and van Saarloos, W., 2004. Weakly nonlinear subcritical instability of visco-elastic Poiseuille flow. J. Non-Newton. Fluid Mech., 116, pp. 235-268.
[64] Morozov, A.N. and Van Saarloos, W., 2007. An introductory essay on subcritical instabilities and the transition to turbulence in visco-elastic parallel shear flows. Physics Reports, 447, pp. 112–143.
[65] Hoda, N., Jovanovic, M.R. and Kumar, S., 2008. Energy amplification in channel flows of viscoelastic fluids. J. Fluid Mech., 601, pp. 407-424.
[66] Xi, L. and Graham, M. D., 2010. Turbulent drag reduction and multistage transitions in viscoelastic minimal flow units. J. Fluid Mech., 647, pp. 421-452.
[67] Zhang, M., Lashgari, I., Zaki, T.A. and Brandt, L., 2013. Linear stability analysis of channel flow of viscoelastic Oldroyd-B and FENE-P fluids. J. Fluid Mech., 737, pp. 249-279.
[68] Samanta, D., Dubief, Y., Holzner, M., Schäfer, C., Morozov, A. N., Wagner, C. and Hof, B., 2013. Elasto-inertial turbulence. PNAS, 110 (26), pp. 10557-10562.
[69] Garg, P., Chaudhary, I., Khalid, M., Shankar, V. and Subramanian, G., 2018. Viscoelastic Pipe Flow is Linearly Unstable. Phys. Rev. Lett., 121, 024502.
[70] Page, J., Dubief, Y. and Kerswell, R.R., 2020. Exact Traveling Wave Solutions in Viscoelastic Channel Flow. Phys. Rev. Lett., 125, 154501.
[71] Morozov, A. and Van Saarloos, W., 2019. Subcritical instabilities in plane Poiseuille flow of an Oldroyd-B fluid. J. Stat. Phys., 175, pp. 554-577.
[72] Shekar, A., McMullen, R. M., McKeon, B. J. and Graham, M.D., 2020. Self-sustained elastoinertial Tollmien–Schlichting waves. J. Fluid Mech., 897, A3.
[73] Chaudhary, I., Garg, P., Subramanian, G. and Shankar, V., 2021. Linear instability of viscoelastic pipe flow. J. Fluid Mech., 908, A11.
[74] Chandra, B., Shankar, V. and Das, D., 2018. Onset of transition in the flow of polymer solutions through microtubes. J. Fluid Mech., 844, pp. 1052-1083.
[75] Wan, D., Sun, G. and Zhang, M., 2021. Subcritical and supercritical bifurcations in axisymmetric viscoelastic pipe flows. J. Fluid Mech., 929, A16.
[76] Sánchez, H.A.C., Jovanović, M.R., Kumar, S., Morozov, A., Shankar, V., Subramanian, G. and Wilson, H.J., 2022. Understanding viscoelastic flow instabilities: Oldroyd-B and beyond. J. Non-Newton. Fluid Mech., 302, 104742.
[77] Buza, G., Page, J. and Kerswell, R.R., 2022. Weakly nonlinear analysis of the viscoelastic instability in channel flow for finite and vanishing Reynolds numbers. J. Fluid Mech., 940, p. A11.
[78] Dong, M. and Zhang, M., 2022. Asymptotic study of linear instability in a viscoelastic pipe flow. J. Fluid Mech., 935, A28.
[79] Datta, S.S., Ardekani, A.M., Arratia, P.E., Beris, A.N., Bischofberger, I., McKinley, G.H., Eggers, J.G., López-Aguilar, J.E., Fielding, S.M., Frishman, A. and Graham, M.D., 2022. Perspectives on viscoelastic flow instabilities and elastic turbulence. Phys. Rev. Fluids, 7(8), p.080701.